Biophysical Chemistry 29 (1988) 17–29
Elsevier

BPC 01210

Approaching the molecular structure of ribosomes

A. Yonath [a,b] and H.G. Wittmann [c]

[a] *Department of Structural Chemistry, Weizmann Institute, Rehovot, Israel,* [b] *Max Planck Research Unit for Structural Molecular Biology, Hamburg, F.R.G. and* [c] *Max Planck Institute for Molecular Genetics, Berlin (West), Germany*

Accepted 15 October 1987

Ribosome; X-ray crystallography; Three-dimensional crystal; Image reconstruction; Subunit tunnel; Heavy-atom cluster

Fifteen forms of three-dimensional crystals and three forms of two-dimensional sheets from ribosomal particles have been grown. In all cases only biologically active particles could be crystallized, the crystalline material retaining its integrity and biological activity for months. Crystallographic data have been collected from crystals of 50 S ribosomal subunits, using synchrotron radiation, at temperatures between 19 and −180 °C. Although at around 0 °C in the synchrotron X-ray beam the crystals rapidly lose their high-resolution reflections, at cryo-temperature hardly any radiation damage occurs over long periods, and a complete set of diffraction data to about 6 Å resolution could be collected from a single crystal. Heavy-atom clusters were used for soaking as well as for specific binding to the surface of the ribosomal subunits prior to crystallization. The 50 S ribosomal subunits from a mutant of *Bacillus stearothermophilus* which lacks the ribosomal protein BL11 crystallize isomorphously with the native form. Models of the entire 70 S ribosome and of the 50 S subunit have been reconstructed from two-dimensional sheets at 47 and 30 Å, respectively. These models demonstrate the overall shape of the particles, the contact areas between large and small subunits, the space where protein biosynthesis may take place and a tunnel through the 50 S subunit which could provide a path for the nascent polypeptide chain.

1. Introduction

It had long been assumed that ribosomes, being flexible, unstable, asymmetric and of enormous size, could not be crytallized. On the other hand, it was found that under stressful conditions such as a cold shock or unsuitable diet, eukaryotic ribosomes form ordered arrays in vivo. The hypothesis that the temporary periodic organization of ribosomes occurs in living organisms when external conditions demand prolonged storage of potentially active ribosomes has led us to initiate crystallographic studies on intact ribosomal particles.

Ribosomes, the cell organelles on which protein biosynthesis takes place, consist of two different subunits which associate upon initiation of the biosynthetic process. Each ribosomal subunit is a defined assembly of proteins and ribonucleic acid chains. A typical bacterial ribosome has a molecular mass of 2.3 MDa. Its large (50 S) subunit is of 1.6 MDa and consists of 32–35 different proteins and two RNA chains. The small subunit (30 S) is of 700 kDa and contains about 21 proteins and one RNA chain.

As a result of an intensive systematic exploration of crystallization conditions and development of an innovative experimental technique for fine control of the volume of the crystallization mixture, procedures for in vitro growth of crystals of intact ribosomal particles have been developed [1–3]. These procedures, combined with sophisticated seeding, proved to be suitable for the reproducible production of ordered three-dimensional crystals and two-dimensional sheets of whole ribosomes as well as of small and large ribosomal subunits. Inactive ribosomal particles could not be

Correspondence address: A. Yonath, Department of Structural Chemistry, Weizmann Institute, Rehovot, Israel.

crystallized. Moreover, in all cases, the crystalline material retains its integrity and biological activity for long periods in spite of the natural tendency of ribosomes to distintegrate and in contrast to the short lifetime of isolated ribosomes in solution.

So far we have obtained 15 different forms of three-dimensional crystals. These include two forms of 70 S ribosomes (from *Escherichia coli* and *Thermus thermophilus* [3–5]); two of the small (30 S) subunits of *Halobacterium marismortui* and *T. thermophilus* [3,5] as well as 11 crystal forms of large (50 S) ribosomal subunits; eight from *Bacillus stearothermophilus* [3,6–12], including particles to which a nascent polypeptide chain and a tRNA molecule are attached [13] and of 50 S subunits of a mutant which lacks one ribosomal protein [14]; and three forms of 50 S subunits from *H. marismortui* [15–17].

Crystals of 50 S subunits from *B. stearothermophilus* and *H. marismortui* are suitable for crystallographic studies. These bacteria are representatives of the eubacteria and archaebacteria, respectively. Thus, we expect that the results of our studies will not only shed light on the structure of ribosomes but also provide information about evolution.

Along with the growth of three-dimensional crystals we produced three forms of ordered two-dimensional sheets: two of native 50 S subunits from *B. stearothermophilus* [18–20], including particles to which a nascent protein and a tRNA molecule are attached [13] and one of 70 S ribosomes from the same bacterial species [21,22]. Three-dimensional image-reconstruction studies have been carried out on sheets of 50 S and 70 S particles [19,22], the results of which are summarized below.

Although ordered three-dimensional crystals and two-dimensional sheets can now be grown from virtually all preparations of active particles, the exact growth conditions for well-ordered crystals must still be varied slightly for each ribosomal preparation, due to the intricate nature of the particles. Moreover, for each crystal form the quality of the crystals depends, in a manner not yet fully characterized, on the procedure used for preparation of the ribosomal subunits and on the strain of a given bacterial species.

In this paper, we describe our crystallographic studies, present results obtained by three-dimensional image reconstruction from two-dimensional sheets and discuss their biological relevance.

2. Experimental

Growth of the different bacterial species, production of their ribosomes and biological characterization are described in refs. 6 and 15. The procedures used for crystal growth and the crystallographic studies are discussed in detail elsewhere [1,2,6,8–12,14–17]. The exact growth conditions are given in the legends to the various figures. Nonspecific derivatization was achieved by soaking crystals in solutions of 2–5 mM heavy-atom cluster for 6–8 h, followed by washing in transfer solutions [2] for 4–6 h. Two-dimensional sheets were grown according to refs. 18–22. The three-dimensional image-reconstruction studies have been described in refs. 19 and 22. For crystallographic studies we used synchrotron radiation at 19, 4, −10, −20 and −180 °C.

Radioactive *N*-ethylmaleimide was reacted with ribosomal particles to determine the accessibility and location of the sulfhydryl groups in ribosomal proteins of the 50 S subunits from *B. stearothermophilus* and *H. marismortui*. An 11-gold cluster and its radioactive derivative were prepared basically following the procedure described in ref. 23. Functional groups were attached to this cluster for covalent binding to ribosomal particles through accessible sulfhydryl groups (S. Weinstein and W. Jahn, manuscript in preparation). The extent of binding of the gold cluster was determined by measuring the radioactivity associated with the 50 S particles as well as by neutron activation (performed at Soreq Nuclear Research Laboratories, Israel). The proteins which bind the cluster and/or *N*-ethylmaleimide were identified by locating the radioactivity on two-dimensional gel electropherograms (S. Weinstein and H.S. Gewitz, manuscript in preparation).

3. Results and discussion

3.1. Crystallographic studies

3.1.1. Large (50 S) ribosomal particles from Bacillus stearothermophilus

Crystals of large ribosomal subunits from *B. stearothermophilus* grow at 4°C either from low-molecular-mass alcohols (fig. 1 and refs. 1, 2, 6 and 8–14), or from low concentrations of polyethylene glycol (fig. 2 and ref. 5). For the latter, the growth solution contained cations that are essential for maintaining the integrity and biological activity of ribosomes at somewhat higher concentrations than those commonly used for storage of the particles or for their crystallization with alcohols [6].

Growing crystals from volatile organic solvents imposes many technical difficulties on manipulation, data collection and heavy-atom derivatization. In fact, any handling of the crystals, such as their removal or reorientation, or replacing the growth medium with a different solution, is detrimental to the crystals. Thus, crystals from the 50 S subunits of wild-type and mutated *B. stearothermophilus* were grown directly in X-ray capillaries. They can reach a length of 2.0 mm and cross-section of 0.4 mm (fig. 1). Since most of the crystals grew with one of their faces adhering to the walls of the capillaries, it was possible to irradiate them without removing the original growth solution. Although the crystals tend to grow with their long axes parallel to the capillary axis, a fair number grow in different directions. Consequently, unit-cell constants have been determined, and diffraction data were obtained without manipulating the crystals. The crystals are loosely packed in an orthorhombic unit cell of 360 × 680 × 920 Å. Fresh crystals diffract to 10–13 Å resolution. However, the higher-resolution reflections decay within 5–10 min. This decay is typical of crystals of ribosomal particles which are irradiated above cryo-temperatures.

Oriented arcs and distinct spots, extending to 3.5 Å resolution, with spacings similar to those measured from diffraction patterns of ribosome gels and extracted rRNA [24–26], have been detected on a few diffraction patterns of single

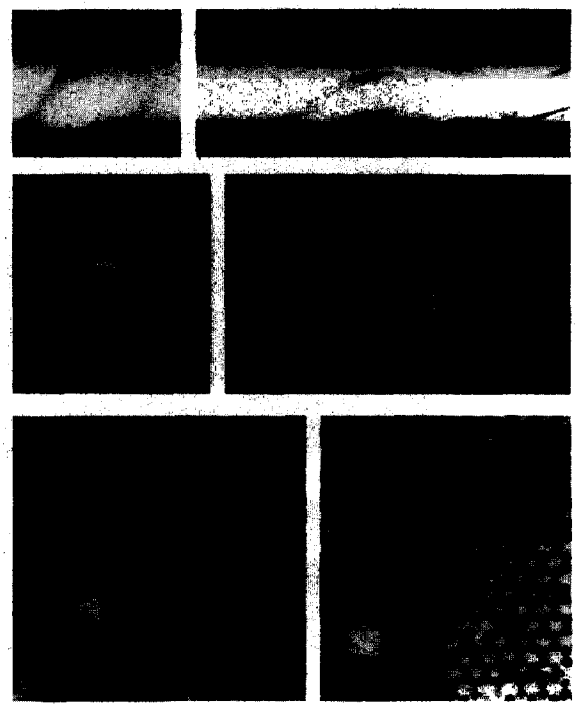

Fig. 1. (a) Crystals of 50 S ribosomal subunits from *B. stearothermophilus* grown in 0.5 mm X-ray capillaries by vapor diffusion at 4°C. Crystallization mixture, 20 μl of 50 S ribosomal subunits (10–20 mg/ml) in H-I buffer [9], 0.01 M spermine, 1% methanol, 10 mM Hepes or glycine buffer (pH 8.4), was equilibrated with a reservoir of 12% methanol, 12% ethylene glycol, 0.5 M NaCl (pH 8.4) (bar = 0.4 mm). (b) X-ray diffraction patterns from crystals similar to those shown in panel a, obtained at −4°C with synchrotron radiation (A1 station at Chess/Cornell University, operating at 5 GeV, current 30–40 mA) with a 0.3 mm collimated X-ray beam of wavelength 1.55 Å, on a Huber precession camera equipped with an He path. Exposure time, 3 min; crystal-to-film distance, 200 mm. (Left) 1° rotation photograph of 0*kl* zone, 680 × 920 Å. (Right) 0.4° rotation photograph of *hk*0 zone, 360 × 680 Å. (c) Electron micrographs of positively stained (2% uranyl acetate) thin sections of crystals similar to those shown in panel a that have been fixed in 0.2% glutaraldehyde and embedded in epon resin (ERL 4206). Optical diffraction patterns are inserted. (Left) Section approximately perpendicular to that shown on the right. Repeat distances measured from optical diffraction: 330 × 1050 Å. This corresponds to the *h*01 zone (360 × 920 Å) in the X-ray patterns (bar = 1000 Å). (Right) Micrograph showing the characteristic open packing of this crystal form. The orthogonal choice of axes corresponds to the 680 × 920 Å zone observed in the X-ray diffraction patterns. Lattice spacing calculated from optical diffraction: 670 × 850 Å.

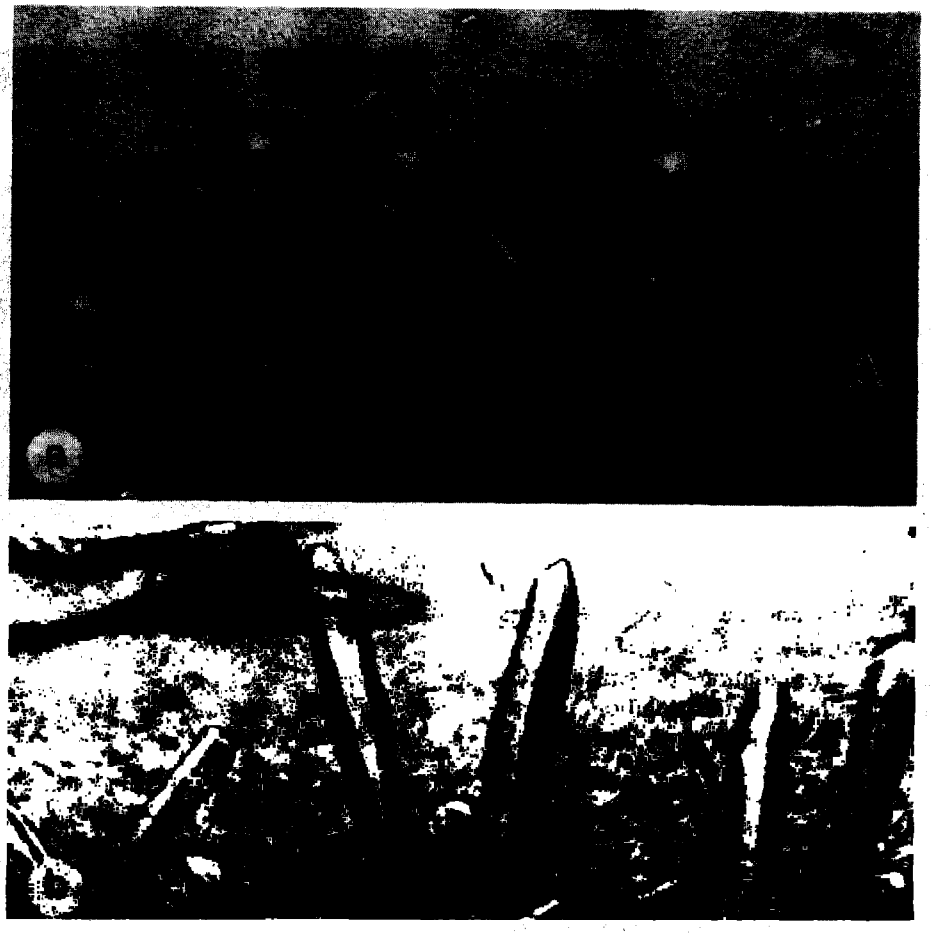

Fig. 2. Crystals of 50 S ribosomal particles from *B. stearothermophilus* grown from polyethylene glycol at 4°C in hanging drops (bar = 0.2 mm). (a) Crystallization solution, at pH 6.4, of 2.5% polyethylene glycol, 0.02 M $(NH_4)_2SO_4$, 0.02 M $MgCl_2$ and 50 S subunits in H-I buffer [9] was equilibrated with a reservoir of 0.15 M KCl together with all other materials in the droplet. (b) Crystallization solution, at pH 6.6, of 2.5% polyethylene glycol, 0.2 M KCl, 0.18 M $(NH_4)_2SO_4$, 0.03 $MgCl_2$ and 50 S particles in H-I buffer [9] was equilibrated with a reservoir of 0.5 M KCl and all materials of the droplet.

crystals and on those of samples containing large numbers of microcrystals. For aligned crystals the average arc length was 60°. These patterns are similar to those observed for nucleosomes [27] and may arise from partial orientation of the nucleic acid component within the particle.

Because crystals of 50 S particles from *B. stearothermophilus* have been grown from polyethylene glycol (fig. 2) very recently, only preliminary crystallographic data are available. These crystals are compactly packed, diffract to about 16 Å resolution, and their X-ray diffraction patterns show periodic spacings of about 260, 320 and 700 Å. Since they have been grown using nonvolatile precipitants, they can be handled. Thus, they may be more suitable for subsequent crystallographic studies. Moreover, our ability to grow crystals of ribosomal particles of eubacteria using precipitants other than alcohols indicates that there is a fair chance that other ribosomal particles from eubacteria can be crystallized in a similar manner. Therefore, efficient crystallographic studies on

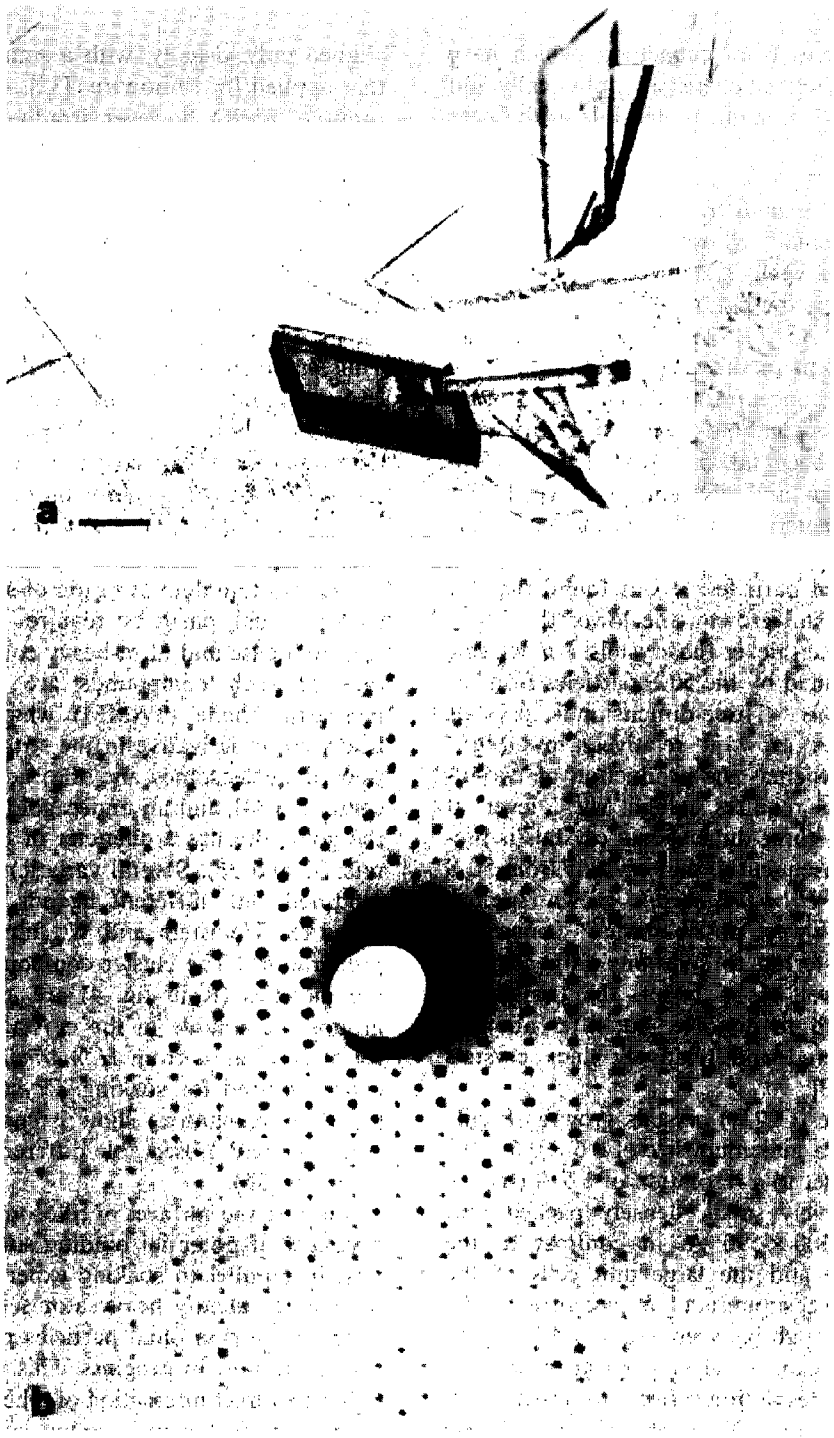

Fig. 3. (a) Crystals obtained from seeds which were grown within 3–5 days from droplets containing 4–5% polyethylene glycol, 1.2 M KCl, 0.5 M NH_4Cl, 0.05–0.10 M $MgCl_2$ and 10 mM spermidine (pH 5.0–5.6) in a crystallization drop containing 5% polyethylene glycol, 1.2 M KCl, 0.5 NH_4Cl, 0.03 M $MgCl_2$, at pH 5.6. This was equilibrated with 7% polyethylene glycol, 1.7 M KCl, 0.5 M NH_4Cl and 0.03 M $MgCl_2$ (pH 5.6) (bar = 0.2 mm). (b) A 1° rotation pattern of a crystal similar to the inserted one. The pattern was obtained at 85 K with synchrotron radiation (7.1 station at SSRL/Stanford University). Wavelength, 1.54 Å; exposure time, 2 min; crystal-to-film distance, 135 mm.

ribosomal particles from eubacteria, which have been well-characterized chemically, physically and biologically [28–31], might be feasible in the near future.

3.1.2. Ribosomal subunits from H. marismortui

Large and small ribosomal subunits from halobacteria have been crystallized in growth solutions which mimic the natural environment within these bacteria [5,15–17]. Thus, KCl, NH_4Cl and $MgCl_2$ are present in the crystallization solution at the minimum concentrations needed for storage of the ribosomes without loss of activity [15]. Advantage has been taken of the delicate equilibrium of mono- and divalent ions needed for growth of halobacteria as well as of the major role played by the Mg^{2+} concentration in crystallization of ribosomal particles. It was found that for spontaneous crystal growth, the lower the Mg^{2+} concentration, the thicker the crystals. An extreme example is provided by the 50 S particles from *B. stearothermophilus*. Three-dimensional crystals from this source grow at relatively low Mg^{2+} concentration, whereas the production of two-dimensional sheets requires a high Mg^{2+} level, at which growth of three-dimensional crystals is prevented [18]. Consequently, thin crystals from 50 S subunits from *H. marismortui*, grown spontaneously at the lowest possible Mg^{2+} concentration, were transferred to solutions with an even lower Mg^{2+} level. As a result, the transferred crystals appeared to dissolve, but after about 2 weeks well-ordered and relatively thick crystals were formed [2,3].

Orthorhombic ($C222_1$) crystals grow as fragile thin plates with a maximum size of $0.6 \times 0.6 \times 0.2$ mm. They diffract to a resolution of 5.5 Å (fig. 3), and have relatively small, densely packed unit cells of $214 \times 300 \times 590$ Å, in contrast to the 'open' structure and the large unit cells of the crystals from 50 S subunits of *B. stearothermophilus* (fig. 1). Although between -2 and 4°C up to 15 photographs can be taken from an individual crystal, the high-resolution reflections appear only on the first two to three X-ray photographs. Hence, over 260 crystals had to be irradiated in order to obtain a complete data set, and X-ray diffraction data were obtained from crystals which had been aligned only visually, with a similar algorithm to that applied for rhino virus [32]. At cryo-temperature (i.e., 85 K), however, irradiated crystals show scarcely any radiation damage for several days. Thus, for the first time, a full data set could be collected from a single crystal.

Moreover, at cryo-temperature the lifetime of the crystals is sufficiently long to allow one to perform preliminary X-ray diffraction experiments using rotating anodes as X-ray generators. Thus, basic parameters such as resolution, unit-cell constants and isomorphism may be determined in the X-ray laboratory, and the progress of structure determination is expected to be less dependent on the availability of synchrotron radiation.

3.1.3. Phase determination

Heavy-atom derivatization of an object as large as ribosomal particles requires the use of extremely dense and ultra-heavy compounds. Examples of such compounds are tetrakis(acetoxymercuri)methane (TAMM) which was the key heavy-atom derivative in the structure determination of nucleosomes and the membrane reaction center [33,34], and an undecagold cluster in which the gold core has a diameter of 8.2 Å (fig. 4 and refs. 35 and 36). Several variations of this cluster, modified with different ligands, have been prepared (S. Weinstein and W. Jahn, manuscript in preparation). The cluster compounds in which all the moieties (R in fig. 4) are amine or alcohol groups are soluble in the crystallization solution for 50 S subunits from *H. marismortui*. Thus, they could be used for soaking. Crystallographic data (to 18 Å resolution) show isomorphous unit-cell constants with observable differences in the intensities (fig. 3b).

Because the surfaces of ribosomal particles have a variety of potential binding sites for such clusters, in parallel to soaking experiments, attempts to bind covalently heavy atoms to a few specific sites on the ribosomal particles prior to crystallization are now in progress. This may be achieved either by direct interaction of a heavy-atom cluster with chemically active groups such as -SH or the ends of rRNA [37] on the intact particles or by the covalent attachment of a cluster to natural or tailor-made carriers which bind specifically to ribosomes.

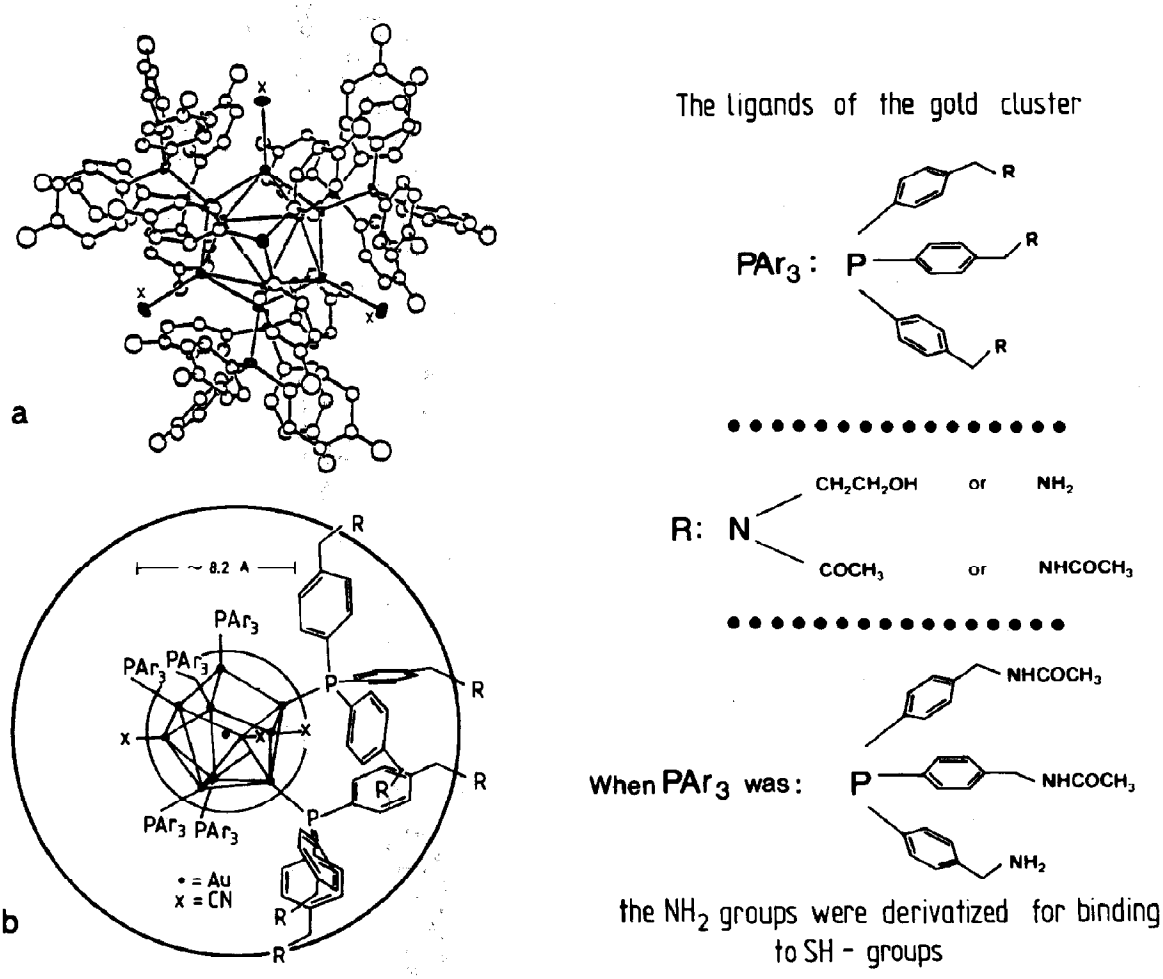

Fig. 4. (a) Postulated molecular structure of the gold cluster used by us based on the crystal structure of a similar cluster. (b) Semi-schematic representation of the gold cluster, depicting the gold core of 8.2 Å diameter and the arrangement of the ligands around it.

For direct binding to the surfaces of ribosomes, the following approaches were taken: Firstly, free sulfhydryls on the surface of the 50 S subunit were located by reaction with radioactive *N*-ethylmaleimide. The labeled proteins were identified by locating the radioactivity in two-dimensional gels. It was found that in the case of 50 S subunits from *B. stearothermophilus* there are mainly two proteins (BL11 and BL13) which bind *N*-ethylmaleimide. For *H. marismortui* a significant portion of the radioactivity was associated with a single protein. Secondly, the gold cluster described above was prepared in such a way that it could be bound to accessible -SH groups. Since this cluster is rather bulky, its accessibility was increased by the insertion of spacers, differing in length, into the cluster as well as into the free -SH groups on the ribosomal particles. Radioactive labeling of this cluster as well as neutron activation analysis of the gold element enabled us to determine the extent of binding of the cluster to the particles. The results of both analytical methods show that a spacer with a minimum length of about 10 Å between the -SH group of a ribosomal protein and

the N atom on the cluster is needed for significant binding. Preliminary experiments indicate that the products of the derivatization reaction with 50 S particles can be crystallized.

As mentioned above, such clusters may also be bound to biochemical carriers. Examples of such carriers are antibiotics [38], DNA oligomers complementary to exposed single-stranded rRNA regions [39] and Fab fragments of antibodies specific to ribosomal proteins. Since most of the interactions of these compounds have been characterized biochemically, the crystallographic location of the heavy-atom compounds will not only be used for phase determination but also reveal the specific functional sites on the ribosome.

Alternatively, such clusters may be attached to selected sites on isolated ribosomal components which will subsequently be incorporated into particles lacking these particular components. Thus, a mutant of *B. stearothermophilus* which lacks protein BL11 was obtained by growing cells in the presence of thiostrepton at 60 ° C (J. Schnier, H.S. Gewitz and B. Leighton, manuscript in preparation). The 50 S mutated ribosomal subunits yield sheets and crystals isomorphous with those of 50 S particles from the wild type [14]. This indicates that BL11, the missing protein, is not involved in crystal forces in the native crystals. Furthermore, protein BL11 has only one sulfhydryl group, and binding of *N*-ethylmaleimide to it does not reduce the biological activity and crystallizability of the particles.

Since protein BL11 is nearly globular [40], its location may be determined in a Patterson map with coefficients of $[F(\text{wild}) - F(\text{mutant})]$ and may serve, by itself, as a giant heavy-atom derivative. At preliminary stages of structure determination this approach may provide phase information and reveal the location of the missing protein.

Along these lines we have adopted a procedure for depleting the ribosomal subunits from several selected proteins [5]. The split proteins were, in turn, incorporated into the depleted core particles and the activity and crystallizability of the reconstituted particles were checked. Preliminary studies reconfirmed the results obtained with the mutant lacking protein BL11. Furthermore, there is a good correlation between the recovery of activity and the ability to crystallize. Thus, particles lacking protein BL12, which are inactive biologically, could not be crystallized, whereas the reconstructed particles produce crystals isomorphous with the native form.

3.2. Three-dimensional image reconstruction

The large size of ribosomal particles, which presents an obstacle to crystallographic studies, permits direct investigation by electron microscopy. Electron microscopy examination of crystalline ribosomal particles may show the location and orientation of particles within the crystals. A model obtained by three-dimensional image reconstruction of two-dimensional sheets may be used for gradual phasing of low-resolution crystallographic data. To this end, we have initiated three-dimensional image reconstruction studies.

Two-dimensional sheets from prokaryotic ribosomal subunits have firstly been grown in vitro from low-molecular-mass alcohols by vapor diffusion in hanging drops [18,42]. Recently, mixtures of salts and alcohols have been used for the rapid growth of better-ordered two-dimensional sheets in depression slides or on electron microscopy grids [19–22].

Well-ordered two-dimensional sheets from 70 S

Fig. 5. (a) Image of a two-dimensional sheet (×28000) of 70 S particles from *B. stearothermophilus* stained with gold-thioglucose, and an optical diffraction pattern from an area containing about 20×15 unit cells. (b) Computer graphic display of the outline of the reconstructed model of the 70 S ribosome at 47 Å resolution stained with gold-thioglucose. L and S indicate the 50 S and 30 S subunits, respectively. The arrows point to the interface between the two subunits (bar = 20 Å). (c) Computer graphic display of the outline of the reconstructed model of the 70 S ribosome at 42 Å resolution stained with uranyl acetate, in a similar orientation to that shown in panel b. UA denotes the regions to which uranyl acetate binds. L and S indicate the 50 S and 30 S subunits, respectively. The arrows point to the interface between the two subunits. Bar = 20 Å. (d) Outline of a 20 Å thick section in the middle of the reconstructed model of the 70 S ribosome. T indicates part of the tunnel. (e) Reconstructed model of the 50 S subunit at 30 Å resolution, obtained as described in fig. 6 and viewed in a projection which resembles models derived from electron microscopy studies of single particles.

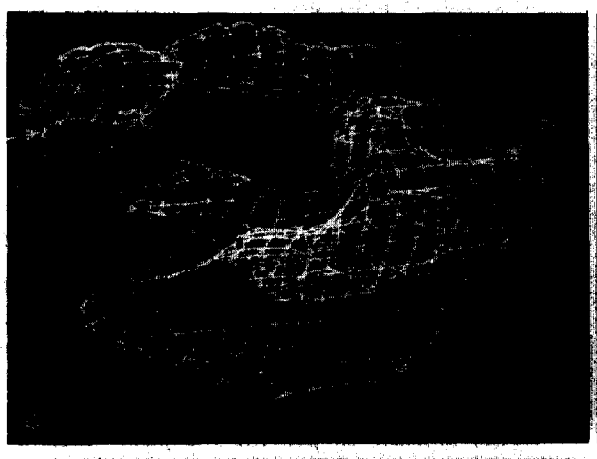

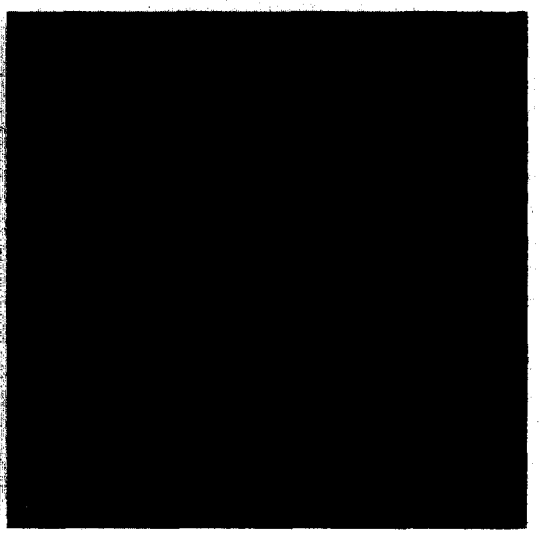

ribosomes and from 50 S ribosomal subunits from *B. stearothermophilus* have been subjected to three-dimensional image reconstruction studies at 47 and 30 Å resolution, respectively [19,20]. In both cases the reconstructed particles have average dimensions similar to those determined using other physical methods [30]. On the basis of the known molecular mass of these particles and of the volume obtained from three-dimensional image reconstruction, the calculated densities are in good agreement with values tabulated [43] and calculated for crystals of the 50 S subunits from *H. marismortui* [17] and other nucleoproteins [44,45].

3.2.1. Two-dimensional sheets of 70 S ribosomes

Two-dimensional sheets of 70 S particles from *B. stearothermophilus* consist of dimers and are packed in relatively small unit cells (about 192 × 420 Å). Analysis of the models obtained by three-dimensional reconstruction of sheets stained with gold-thioglucose demonstrates the two ribosomal subunits. These are arranged around an empty space which is large enough to accommodate the components of protein biosynthesis, e.g., tRNAs and elongation factors. There is a similarity between the model of the small subunit obtained by visualization of single particles [30] and that revealed by our studies. However, isolated 30 S particles appear somewhat wider than those reconstructed within the 70 S particles. This may be a consequence of contact of the isolated particles with the flat electron microscope grid. In contrast, particles within the crystalline sheets are held together by crystalline forces. These form a network which may stabilize the conformation of the particle and diminish or even eliminate the influence of the flatness of the grids. The portion of the reconstructed 70 S particle which we assigned to the large subunit may be correlated to the image that we reconstructed from two-dimensional sheets of these subunits (fig. 5 and ref. 19).

Reconstruction from sheets of 70 S ribosomes stained with uranyl acetate led to a model which showed the features described above as well as regions where uranyl acetate, acting as a positive stain, was incorporated into the particle. This may indicate that in these regions the RNA which is the natural candidate for interacting with uranyl acetate is concentrated and exposed to the stain. Such regions are located on the body of the small subunit [46] and at the interface of the small and large subunits, in good agreement with other studies [47].

3.2.2. Two-dimensional sheets of 50 S ribosomal subunits

The two-dimensional sheets of the 50 S subunits consist of small unit cells, (around 140 × 330 Å). Optical diffraction patterns of electron micrographs of negatively stained specimens with gold-thioglucose extend to about 30 Å. Three-dimensional image reconstruction of these sheets yielded a model showing several projecting arms, two of which are longer than the rest. The arms are arranged radially around one edge near the presumed interface with the 30 S subunit. A narrow elongated cleft is formed between the projecting arms and turns into a tunnel of diameter up to 25 Å and 100–120 Å length (fig. 6). A similar feature was also detected on ribosomes from chick embryos by three-dimensional image reconstruction [47].

The functional significance of the tunnel remains to be determined. However, this tunnel, originating at the presumed site of actual protein biosynthesis and terminating on the other end of the particle, and being of a diameter large enough to accommodate a peptide of about 40 amino acids, appears to provide the path taken by the nascent polypeptide chain. Protection by the ribosome of newly formed peptides of about 40 amino acids from proteolytic enzymes was previously observed using biochemical methods [48–50]. It remains to be seen whether the tunnel terminates at a location compatible with that assigned by immunoelectron microscopy as the exit site for the growing polypeptide chain [51].

The tunnel is present in all reconstructions that we have performed, irrespective of the staining material (gold-thioglucose or uranyl acetate). In every reconstructed particle there is a region of low density which branches off the tunnel to form a Y (or V) shape and terminates on the opposite side of the particle (fig. 6). As yet, the exact nature of this region cannot be determined. It may be a loosely packed protein region, but in some recon-

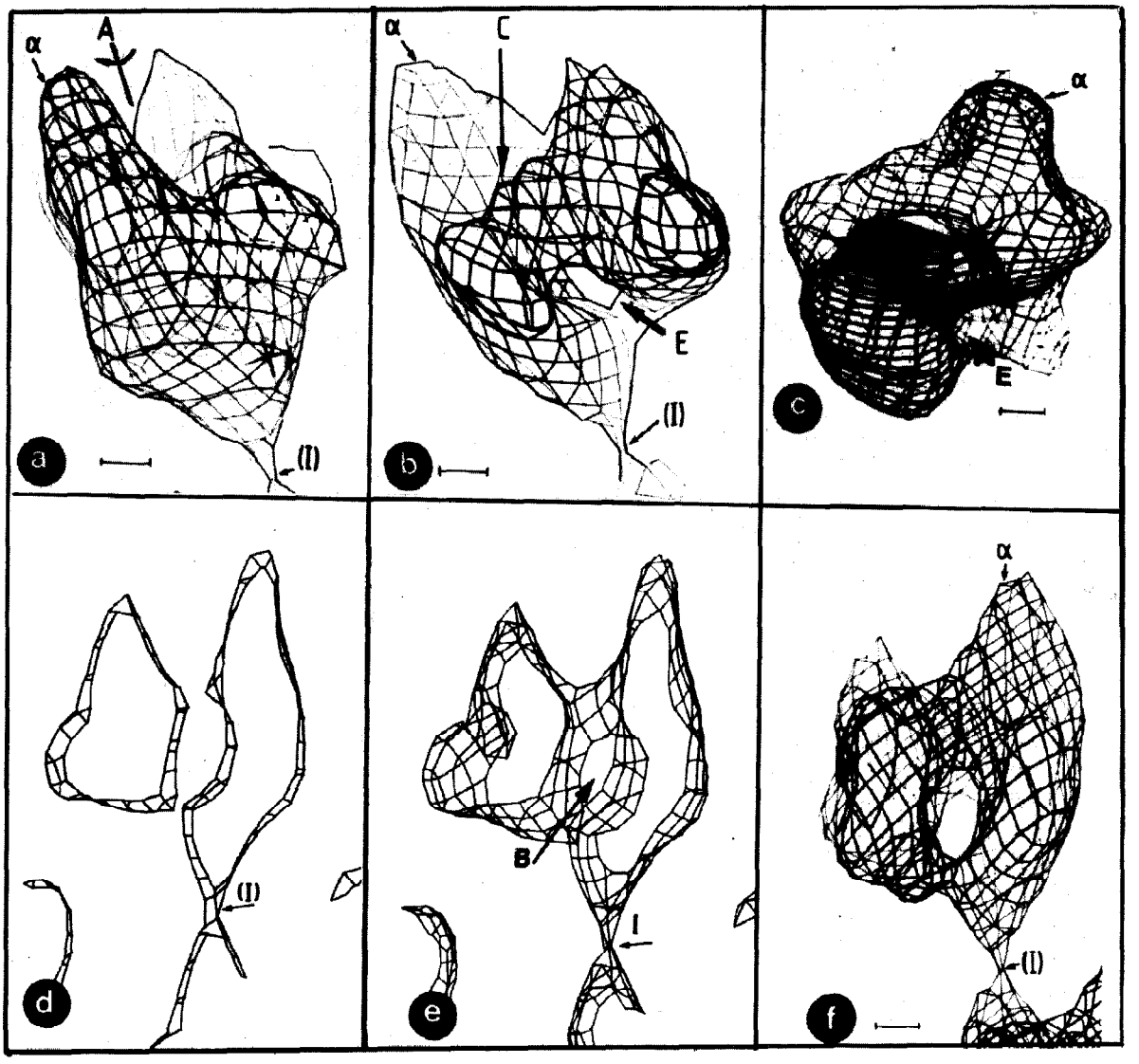

Fig. 6. Computer graphic display of the reconstructed model of the 50 S ribosomal subunit at 30 Å resolution. α denotes the longest arm; E indicates the exit site. (a) Side view of the model. The entire particle and part of a second one are shown. The arrow (I) points to the crystal contact between the two particles. A marks the approximate axis around which the model was turned to obtain the view shown in panel b (bar = 20 Å). (b) The model shown in panel a rotated about the axis A. C indicates the cleft between the projecting arms, at the site where it turns into the tunnel. (c) View into the tunnel from the cleft. (d) Outline of a 20 Å thick section in the middle of the reconstructed model, showing that the tunnel spans the entire particle. (e) Outline of a 40 Å thick section in the middle of the reconstructed model. The branching of the tunnel is seen (B). (f) Model viewed into the branch of the tunnel from the exit point.

structed models the density of this region is so low that it appears as a branch of the main tunnel.

Several models for the 50 S ribosomal subunits from *E. coli* have previously been suggested based on electron microscopical visualization, reconstruction or averaging of single particles [30]. Our model can be positioned in such a manner that its projected view resembles the usual image seen

when single particles are investigated by electron microscopy (fig. 5). However, there are some discrepancies between our model and the others, i.e., ours does not have any flat surface. These, as in the case of 70 S particles, may stem from the basic differences between the subjective visualization of isolated particles in projection on the one hand, and the inherently more objective character of structure analysis by diffraction methods on the other.

In the reconstructed 70 S ribosomes from *B. stearothermophilus* there are some indications for the existence of a tunnel. Thus, portions of the tunnel could be detected in 20–40 Å thick sections through the particle. An example is shown in fig. 5. Since the 70 S particles used for these studies were harvested at the time of being active, it is feasible that nascent protein chains were attached to them. This may be the reason for the fact that the tunnel is only partially resolved.

4. Concluding remarks

We have demonstrated here that crystallographic studies may be carried out on intact ribosomal particles. We expect that these studies supported by electron microscopy and combined with available biophysical, biochemical and genetic knowledge will yield a reliable model for the ribosome and contribute to an understanding of the mechanism of protein biosynthesis at the molecular level.

Acknowledgements

We would like to thank Dr. H. Hope for introducing cryo-temperature crystallography, Drs M.A. Saper, K.S. Bartels, C. Kratky, G. Weber, Ms. P. Webster and Mr. K. von Buhlen for their efforts in data collection, Dr. K.R. Leonard and Mr. T. Arad for their contribution to the image reconstruction studies, Drs. S. Weinstein, W. Jahn and K. Amornajurasi for their work on the heavy-atom derivatization, Dr. F.L. Hirshfeld for his critical comments, Drs J. Sussman and B. Shaanan for assisting us with computing and display problems, Drs K. Wilson, H.D. Bartunik, J. Helliwell, M. Papiz, K. Moffat, W. Schildcamp, P. Pizackerley and E. Merrit for providing synchrotron radiation facilities, and H.S. Gewitz, J. Piefke, Y. Halfon, B. Romberg, G. Idan and H. Danz for technical assistance. This work was supported by BMFT (05 180 MP B0), NIH (GM 34360) and Minerva research grants.

References

1 A. Yonath, J. Müssig and H.G. Wittmann, J. Cell Biochem. 19 (1982) 145.
2 A. Yonath and H.G. Wittman, Methods Enzymol. (1988) in the press.
3 A. Yonath, F. Frolow, M. Shoham, J. Müssig, I. Makowski, C. Glotz, W. Jahn, S. Weinstein and H.G. Wittmann, J. Crystal Growth (1987) in the press.
4 H.G. Wittmann, J. Müssig, H.S. Gewitz, J. Piefke, H.J. Rheinberger and A. Yonath, FEBS Lett. 146 (1982) 217.
5 C. Glotz, J. Müssig, H.S. Gewitz, I. Makowski, T. Arad, A. Yonath and H.G. Wittmann, Biochem. Int. 15 (1987) 953.
6 A. Yonath, J. Müssig, B. Tesche, S. Lorenz, V.A. Erdmann and H.G. Wittmann, Biochem. Int. 1 (1980) 428.
7 A. Yonath, Trends Biochem. Sci. 9 (1984) 227.
8 A. Yonath, H.D. Bartunik, K.S. Bartels and H.G. Wittmann, J. Mol. Biol. 177 (1984) 201.
9 A. Yonath, M.A. Saper, I. Makowski, J. Müssig, J. Piefke, H.D. Bartunik, K.S. Bartels and H.G. Wittmann, J. Mol. Biol. 187 (1986) 633.
10 A. Yonath, M.A. Saper and H.G. Wittmann, in: Structure, function and genetics of ribosomes, eds. B. Hardesty and G. Kramer (Springer-Verlag, Heidelberg, 1986) p. 112.
11 A. Yonath, K.R. Leonard, S. Weinstein and H.G. Wittmann, Cold Spring Harbor Symp. (1987) in the press.
12 A. Yonath and H.G. Wittmann, Proceedings of the 5th Albany conversation, ed. M. Sarma (Adenine Press, Albany, NY, 1987) in the press.
13 H.S. Gewitz, C. Glotz, J. Müssig, J. Piefke, A. Yonath and H.G. Wittmann, Biochimie (1987) in the press.
14 A. Yonath, M.A. Saper, F. Frolow, I. Makowski and H.G. Wittmann, J. Mol. Biol. 192 (1986) 161.
15 A. Shevack, A., H.S. Gewitz, B. Hennemann, A. Yonath and H.G. Wittmann, FEBS Lett. 184 (1985) 68.
16 M. Shoham, J. Müssig, A. Shevack, T. Arad, H.G. Wittmann and A. Yonath, FEBS Lett. 208 (1986) 321.
17 I. Makowski, F. Frolow, M.A. Saper, H.G. Wittmann and A. Yonath, J. Mol. Biol. 193 (1987) 819.
18 T. Arad, K.R. Leonard, H.G. Wittmann and A. Yonath, EMBO J.3. (1984) 127.
19 A. Yonath, K.R. Leonard and H.G. Wittmann, Science 236 (1987) 813.
20 T. Arad, J. Piefke, H.S. Gewitz, B. Romberg, C. Glotz, J. Müssig, A. Yonath and H.G. Wittmann, Anal. Biochem. (1987) in the press.

21 J. Piefke, T. Arad, I. Makowski, H.S. Gewitz, B. Hennemann, A. Yonath and H.G. Wittmann, FEBS Lett. 209 (1986) 104.
22 T. Arad, J. Piefke, S. Weinstein, H.S. Gewitz, A. Yonath and H.G. Wittmann, Biochimie (1987) in the press.
23 P.A. Bartlett, B. Bauer and S.J. Singer, J. Am. Chem. Soc. 100 (1978) 5085.
24 A. Klug, K.C. Holmes and J.T. Finch, J. Mol. Biol. 3 (1961) 87.
25 G. Zubay and M.H.F. Wilkins, J. Mol. Biol. 2 (1960) 105.
26 R. Langridge and K.C. Holmes, J. Mol. Biol. 5 (1962) 611.
27 J.T. Finch, L.C. Lutter, D. Rhodes, R.S. Brown, B. Rushton, M. Levitt and A. Klug, Nature 269 (1977) 29.
28 G. Chambliss, G.R. Craven, J. Davies, L. Kahan and M. Nomura, Ribosomes: structure, function and genetics (University Park Press, Baltimore, 1980).
29 H.G. Wittmann, Annu. Rev. Biochem. 51 (1982) 155.
30 H.G. Wittmann, Annu. Rev. Biochem. 52 (1983) 35.
31 B. Hardesty and G. Kramer, Structure, function and genetics of ribosomes (Springer-Verlag, Heidelberg, 1986).
32 M.G. Rossmann and W. Erickson, J. Appl. Crystallogr. 16 (1983) 629.
33 J. Deisenhofer, O. Epp, K. Mikki, R. Huber and H. Michel, J. Mol. Biol. 180 (1984) 385.
34 T. Richmond, J.T. Finch, B. Rushton, D. Rhodes and A. Klug, Nature 311, (1984) 533.
35 P. Bellon, P.M. Manassero and M. Sansoni, J. Chem. Soc. Dalton. Trans. (1972) 1481.
36 J.S. Wall, J.F. Hainfeld, P.A. Barlett and S.J. Singer, Ultramicroscopy 8 (1982) 397.
37 O.W. Odom, Jr, D.R. Robbins, J. Lynch, D. Dottavio-Martin, G. Kramer and B. Hardesty, Biochemistry 19 (1980) 5941.
38 K.H. Nierhaus and H.G. Wittmann, Naturwissenschaften 67 (1980) 234.
39 W.E. Hill, B.E. Trappich and B. Tassanakajohn, in: Structure, function and genetics of ribosomes, eds. B. Hardesty and G. Kramer (Springer-Verlag, Heidelberg, 1986) p. 233.
40 L. Giri, W.E. Hill, H.G. Wittmann and B. Wittmann-Liebold, Adv. Protein Chem. 36 (1984) 1.
41 H.-S. Gewitz, C. Glotz, P. Goischke, B. Romberg, A. Yonath and H.G. Wittmann, Biochem. Int. 15 (1987) 1887.
42 M.W. Clark, K.R. Leonard and J.A. Lake, Science 216 (1982) 999.
43 B.W. Matthews, J. Mol. Biol. 33 (1968) 491.
44 J.M. Hogle, J. Mol. Biol. 160 (1982) 663.
45 L. Liljas, T. Unge, A. Jones, K. Fridborg, S. Lovgren, U. Skoglund and B. Strandberg, J. Mol. Biol. 159 (1982) 93.
46 R. Brimacombe, J. Atmadja, W. Stiege and D. Schüler, J. Mol. Biol. 199 (1988) 115.
47 R.A. Milligan and P.N.T. Unwin, Nature 319 (1986) 693.
48 L.I. Malkin and A. Rich, J. Mol. Biol. 26 (1967) 329.
49 G. Blobel and D.D. Sabatini, J. Cell Biol. 45 (1970) 130.
50 W.P. Smith, P.C. Tai and B.D. Davis, Proc. Natl. Acad. Sci. U.S.A. 75 (1978) 5922.
51 C. Bernabeau and J.A. Lake, Proc. Natl. Acad. Sci. U.S.A. 79 (1982) 3111.